RESEARCH COMMUNICATION

Biofactors WILEY

Treatment of the metabolic syndrome by siRNA targeting apolipoprotein CIII

Patricia Recio-López[1]　｜　Ismael Valladolid-Acebes[1]　｜　Philipp Hadwiger[2]　｜
Markus Hossbach[2]　｜　Monika Krampert[2]　｜　Carla Prata[2]　｜　Per-Olof Berggren[1]　｜
Lisa Juntti-Berggren[1]

[1]The Rolf Luft Research Center for Diabetes and Endocrinology, Karolinska Institutet, Karolinska University Hospital L1, Stockholm, Sweden
[2]Axolabs GmbH, Kulmbach, Germany

Correspondence
Ismael Valladolid-Acebes and Lisa Juntti-Berggren, The Rolf Luft Research Center for Diabetes and Endocrinology, Karolinska Institutet, Karolinska University Hospital L1, SE-171 76 Stockholm, Sweden.
Email: Ismael.valladolid.acebes@ki.se and lisa.juntti-berggren@ki.se

Abstract
Apolipoprotein CIII (apoCIII) is increased in obesity-induced insulin resistance and type-2 diabetes. Emerging evidences support the advantages of small interfering RNAs (siRNAs) to target disease-causing genes. The aim of this study was to develop siRNAs for in vivo silencing of apoCIII and investigate if this results in metabolic improvements comparable to what we have seen using antisense oligonucelotides against apoCIII. Twenty-four siRNAs were synthesized and tested in a dual luciferase reporter assay. The eight best were selected, based on knockdown at 20 nM, and of these, two were selected based on IC_{50} values. In vivo experiments were performed in *ob/ob* mice, an obese animal model for diabetes. To determine the dose-dependency, efficacy, duration of effect and therapeutic dose we used a short protocol giving the apoCIII-siRNA mix for three days. To evaluate long-term metabolic effects mice were treated for three days, every second week for eight weeks. The siRNA mix effectively and selectively reduced expression of apoCIII in liver in vivo. Treatment had to be repeated every two weeks to maintain a suppression of apoCIII. The reduction of apoCIII resulted in increased LPL activity, lower triglycerides, reduced liver fat, ceased weight gain, enhanced insulin sensitivity, and improved glucose homeostasis. No off-target or side effects were observed during the eight-week treatment period. These results suggest that in vivo silencing of apoCIII with siRNA, is a promising approach with the potential to be used in the battle against obesity-induced metabolic disorders.

Abbreviations: ACC, acetyl-co-enzyme A carboxylase; ALT, alanine aminotransferase; Angptl, angiopoietin-like-peptide; Apo, apolipoprotein; ASO, antisense oligonucleotide; AST, aspartate aminotransferase; ATGL, adipose triglyceride lipase; ChREBP, carbohydrate-responsive element binding protein; Cpt-1a, carnitine palmitoyltransferase 1a; Ct, cycle threshold; DLS, dynamic light scattering; FAS, fatty acid synthase; GSIS, glucose-stimulated insulin secretion; HDL, high-density lipoprotein; HFD, high fat diet; HNF-4, hepatic nuclear factor-4; HSL, hormone-sensitive lipase; IPGTT, intraperitoneal glucose tolerance test; IRE, insulin/phorbol ester responsive element; LDL, low-density lipoprotein; LDL-R, low-density lipoprotein receptor; LNP, lipid nanoparticle; LPL, lipoprotein lipase; LRP-1, low-density lipoprotein receptor-related protein 1; miRNAs, micro-RNAs; PDI, polydispersity index; PVS, polyvinyl sulfonic acid; RNAi, RNA-interference; siRNAs, small interfering RNAs; SREBP-1, sterol regulatory element-binding protein 1; TF, transferrin; Tgs, triglycerides; TRL, triglyceride-rich lipoprotein.

Patricia Recio-López and Ismael Valladolid-Acebes contributed equally to this work.

1 | INTRODUCTION

Apolipoprotein CIII (apoCIII) is associated with triglyceride-rich lipoproteins (TRL), low-density (LDL), and high-density (HDL) lipoproteins and has an important role in lipid metabolism.[1–3] It has long been known that increased levels of apoCIII is an independent risk factor for cardiovascular diseases (CVD) and the underlying mechanisms involve inhibition of lipoprotein lipases (LPL) and hepatic clearance of TRL as well as pro-inflammatory causes.[4–8] ApoCIII is also of interest in obesity, insulin-resistance and diabetes.[9–12] Among several other pathways, glucose and insulin affect the expression of the apoCIII gene.[13–15] Insulin suppresses, via inhibition of the insulin/phorbol ester responsive element (IRE) within the apoCIII gene,[14,16,17] while glucose stimulates the expression of the apoCIII gene through hepatic nuclear factor-4 (HNF-4) and carbohydrate-responsive element binding protein (ChREBP).[15] Therefore, hyperglycemia together with insulin deficiency in type-1 diabetes (T1D), and insulin resistance in type-2 diabetes (T2D), are related to increased levels of apoCIII.[14,15,17,18]

In animal models of obesity and diabetes, and in humans, decreasing apoCIII by antisense oligonucleotides (ASO) leads to metabolic improvements.[12,19-22] We have demonstrated that high-fat diet (HFD) induced obesity, liver steatosis, insulin resistance and diabetes can be prevented if mice are treated with ASO against apoCIII directly from start of the diet. It was also possible to reverse the metabolic derangements in mice that were first fed HFD for 10 weeks and then given ASO against apoCIII.[22]

The degree of apoCIII suppression needed to induce metabolic protective effects ranges from 40 to 98%, depending on species, strains, diets and genetic factors.[12,20,21] Important to note is that a total lack of apoCIII causes a more pronounced HFD-induced obesity and insulin resistance.[23]

Statins, fibrates, omega-3 carboxylic acids and peroxisome proliferator-activated receptor alpha (PPAR-α) agonists are clinically used drugs that have been reported to reduce apoCIII. However, the observed effects on apoCIII by these drugs are very moderate compared to the reduction obtained by ASO.[12,20,21,24]

Another method to target specific genes is the robust siRNA technology. There are some evidences, although mostly from in vitro experiments, that it might be more potent than ASO.[25–29] Therefore, the aim of this study was to develop siRNAs targeting mouse liver apoCIII and in vivo test the effects in obese, insulin resistant type-2 diabetic *ob/ob* mouse.

2 | METHODS

2.1 | Design and synthesis of siRNA

siRNAs with asymmetric structures were designed in silico based on the full-length mouse apoCIII mRNA transcript variant NM_023114.4 and perfectly matched also to other mRNA transcript variants from NCBI release 87 and Ensembl release 92 (NM_001289755.1, NM_001289756.1, NM_001289833.1, ENSMUST00000121916, ENSMUST00000034586, ENSMUST00000214729). The siRNA guide strands used in this study were designed to be a perfect match only to their target mRNA and to have at least two mismatches within positions 2–18 of the 19mer guide strand sequence to any other transcript from the NCBI (Ref Seq database, release 87). The number of off-target genes that are hit with two mismatches should be as small as possible (e.g., ≤20). The siRNA guide strands lacked a seed region (nucleotides 2–7) identical with seed regions of known mouse miRNAs (miRBase, release 21). To optimize the thermodynamic profile, the sequences of both strands were edited. An adenine was placed at position 19 of the passenger strand and an uracil was used at position 1 of the guide strand. siRNA specificity and activity were predicted with proprietary algorithms (Axolabs GmbH). Twenty-four siRNAs that best met the criteria for specificity and activity were selected for synthesis. Chemically modified siRNAs for mouse apoCIII and a control siRNA (firefly luciferase) listed in Table 1 were synthesized by Axolabs, as described previously.[30]

2.2 | Cell culture and in vitro screening

Hepa1-6 cells from ATCC were cultivated in Dulbecos modified Eagle's Medium supplemented with 10% fetal bovine serum (FBS), 100 U ml⁻¹ penicillin and 100 mg ml⁻¹ streptomycin. For evaluation of siRNA potency, the cell-based DualGlo reporter assay system (Promega) was used. Briefly, the full murine apoCIII target sequence (NM_023114.4, 527 bp) was cloned into

TABLE 1 Sequences of the different apoCIII-siRNAs used in the current study

Target	Duplex-ID	Sense sequence	Antisense sequence
ApoCIII	XD-11455	gguAGAGGGAuccuuGcuAs(invdT)	uAGcAAGGAUCCCUCuACCusu
ApoCIII	XD-11456	gaAcAAGccuccAaGAcGAs(invdT)	UCGUCUUGGAGGCUUGUUUCusu
ApoCIII	XD-11457	ccAGGAuGcGcuAaGuAGAs(invdT)	UCuACUuAGCGcAUCCUGGusu
ApoCIII	XD-11458	caGGAuGcGcuAAguAGcAs(invdT)	UGCuACUuAGCGcAUCCUGusu
ApoCIII	XD-11459	ggAuGcGcuAAGuaGcGuAs(invdT)	uACGCuACUuAGCGcAUCCusu
ApoCIII	XD-11460	gcuAAGuAGcGuGcAGGAAs(invdT)	UUCCUGcACGCuACUuAGCusu
ApoCIII	XD-11461	aguccGAuAuAGcuGuGGAs(invdT)	UCcAcAGCuAuAUCGGACUusu
ApoCIII	XD-11462	cuGGAuGGAcAAucAcuuAs(invdT)	uAAGUGAUUGUCcAUCcAGusu
ApoCIII	XD-11463	ugGAcAAucAcuucAGAuAs(invdT)	uAUCUGAAGUGAUUGUCcAusu
ApoCIII	XD-11464	ggAcAAucAcuucaGAucAs(invdT)	UGAUCUGAAGUGAUUGUCCusu
ApoCIII	XD-11465	cuucAGAucccuGaAAGGAs(invdT)	UCCUUUcAGGGAUCUGAAGusu
ApoCIII	XD-11466	ggcuAcuGGAGcAaGuuuAs(invdT)	uAAACUUGCUCcAGuAGCCusu
ApoCIII	XD-11467	cuGGAGcAAGuuuacuGAAs(invdT)	UUcAGuAAACUUGCUCcAGusu
ApoCIII	XD-11468	gaGcAAGuuuAcugAcAAAs(invdT)	UUUGUcAGuAAACUUGCUCusu
ApoCIII	XD-11469	caAGuuuAcuGAcaAGuuAs(invdT)	uAACUUGUcAGuAAACUUGusu
ApoCIII	XD-11470	cuGAcAAGuucAccGGcuAs(invdT)	uAGCCGGUGAACUUGUcAGusu
ApoCIII	XD-11471	ccAAccAAcuccAgcuAuAs(invdT)	uAuAGCUGGAGUUGGUUGGusu
ApoCIII	XD-11472	cuccAGcuAuuGAgucGuAs(invdT)	uACGACUcAAuAGCUGGAGusu
ApoCIII	XD-11473	ccAGcuAuuGAGucGuGAAs(invdT)	UUcACGACUcAAuAGCUGGusu
ApoCIII	XD-11474	cccuAGAucucAccuAAAAs(invdT)	UUUuAGGUGAGAUCuAGGGusu
ApoCIII	XD-11475	cucAccuAAAcAugcuGuAs(invdT)	uAcAGcAUGUUuAGGUGAGusu
ApoCIII	XD-11476	cauGcuGucccuAauAAAAs(invdT)	UUUuAUuAGGGAcAGcAUGusu
ApoCIII	XD-11477	ccuAAuAAAGcuGgAuAAAs(invdT)	UUuAUCcAGCUUuAUuAGGusu
ApoCIII	XD-11478	uaAuAAAGcuGGAuAAGAAs(invdT)	UUCUuAUCcAGCUUuAUuAusu
Fluc	XD-00194	cuuAcGcuGAGuAcuucGAdTsdT	UCGAAGuACUcAGCGuAAGdTsdT

Note: For each sequence capital letters mean RNA, lower cases mean 2′-O-methyl modified RNA, s means phosphorothioate; dT means deoxythymidine, and invdT means inverted deoxythymidine.

the 3′UTR of the Renilla luciferase gene in the psiCheck-2 vector, allowing the expression of a Renilla-luciferase-ApoCIII fusion protein together with an independently expressed firefly-luciferase from the same plasmid. Hepa1-6 cells were co-transfected with the reporter plasmid and the siRNAs of interest using Lipofectamine2000 (Thermo) as transfection reagent and incubated for 24 h at 37°C and 5% CO_2. Activity of both luciferases was measured using the DualGlo reagent system (Promega) in a Victor Light luminescence plate reader (PerkinElmer). For analysis of knockdown activity, luminescence units obtained for Renilla luciferase were first normalized to the firefly signal. Relative luciferase activity measured with control-treated cells were set as 1, and relative activity values were calculated for the siRNA treated cell samples. For dose–response experiments, the XLfit software (IBDS) was used to calculate IC_{50} values. Dose–response curves are presented

using a semi-logarithmic plot and analyzed by non-linear regression modeling.

2.3 | LNP formulation and RNA encapsulation

1,2-Distearoyl-3-phosphatidylcholine (DSPC) and 1,2-dimyristoyl-rac-glycero-3-methylpolyoxyethylene (PEG2000-DMG) were purchased from NOF Europe GmbH (Frankfurt am Main, Germany). Cholesterol was obtained from Sigma–Aldrich (Taufkirchen, Germany). The lipid nanoparticle (LNP) components were dissolved in 100% ethanol and mixed to yield the following molar ratios: 50% XL10 lipid, 10% DSPC, 38.5% cholesterol, and 1.5% PEG2000-DMG. siRNA stock solution was prepared in 50 mmol L^{-1} sodium citrate buffer, pH 3, at concentration of 0.5 mg ml^{-1}. LNPs were formed by

microfluidic mixing of the siRNA and lipid solutions at 3:1 volumetric ratio using a Precision Nanosystems NanoAssembler benchtop Instrument. After mixing, the LNPs were collected and the buffer was exchanged with phosphate-buffered saline (PBS) (200-fold excess of sample volume) overnight at room temperature under stirring using a 10 kDa Slide-a-Lyzer G2 Dialyses cassette (Thermo Fisher Scientific). The resulting nanoparticle suspension was filtered through 0.2 μm sterile filter into glass vials. The LNPs were characterized for size, polydipsersity index (PDI), zeta potential using a DLS Malvern zetasizer nano and encapsulation efficiency using a modified Quant-iT™ RiboGreen® RNA assay. The nanoparticles were diluted in PBS, the size and PDI of the particles were measured by dynamic light scattering (DLS) technique using a Zetasizer Nano ZSP, ZEN5600, Malvern Instruments Ltd., UK with, He–Ne laser ($\lambda = 633$ nm). The results are the average of the triplicate measurements and expressed as z-average diameter and PDI. Zeta potential of nanoparticles was measured by the same Zetasizer using M3-PALS technique. The results are the average of the triplicate measurements and expressed as zeta potential.

The samples were diluted to a concentration of approximately 5 ng ml^{-1} in Tris-EDTA (TE) buffer pH 7.5. 50 μl of the diluted samples were transferred to a polystyrene 96 well plate, then either 50 μl of TE buffer (measuring unencapsulated RNA) or 50 μl of a 2% Triton X-100 solution (measuring total RNA, both encapsulated within LNPs and un-encapsulated, "free" RNA) was added. Samples were prepared in triplicate. The plate was incubated for 15 min at a temperature of 37°C. The RiboGreen reagent was diluted 1:100 in TE buffer, 100 μl of this solution was added to each well. The fluorescence intensity was measured using a fluorescence plate reader (Wallac Victor 1420 Multilabel Counter; Perkin Elmer, Waltham, MA) at an excitation wavelength of approximately 480 nm and an emission wavelength of approximately 520 nm. The fluorescence values of the reagent blank were subtracted from that of each of the samples and the encapsulation efficiency was determined as follows:

$$\text{encapsulation efficiency} = \left(1 - \frac{\text{uncapsulated RNA}}{\text{total RNA}}\right) \times 100$$

2.4 | In vivo studies

2.4.1 | Selection, synthesis and formulation of siRNAs for in vivo studies

The two siRNAs with lowest IC$_{50}$ values were synthesized by Axolabs GmbH and an equimolar mix of both was formulated in LNPs for intravenous injections (i.v.), using the Axolabs proprietary cationic lipid XL10 (LGC Axolabs GmbH, Germany).[31] The use of this liposomal formulation was selected because it has been demonstrated to result in liver-specific knockdown of target genes without significant effects in other tissues.[32–34] The active siRNA mix against mouse apoCIII gene was prepared at a concentration of 0.55 mg ml^{-1} and will be referred to as apoCIII-siRNA mix. The concentration of the chemically inactivated siRNA (XD-00194 oligo), directed against firefly luciferase[30] and used as control, was 0.54 mg ml^{-1}.

2.4.2 | Animals

All animal care and experiments were carried out according to the Animal Experiment Ethics Committee at Karolinska Institutet.

Male and female B6.Cg-Lep^{ob}/ Lep^{ob}J (*ob/ob*) mice on a C57BL6/j background from our own breeding colony at Karolinska Institutet were used. They were 12 weeks of age at start of the experiments. Animals were housed 3–5 per cage in a temperature- and humidity-controlled room with 12 h light/dark cycles. To test whether this siRNA mix against mouse apoCIII also recognizes rat apoCIII we used 40 days old male and female diabetes-prone (DP) BioBreeding (BB) rats from our own breeding colony at Karolinska Institutet. Rats were housed under specific pathogen-free conditions in a temperature- and humidity-controlled room with 12 h light/dark cycles. All animals were fed R70 chow diet (Lantmännen, Sweden) and water ad libitum.

2.4.3 | In vivo concentration-response curves

One day before injection of the siRNAs, body weight (BW) and blood glucose (BG) were determined under non-fasting conditions to randomize and assign the mice to three different groups: (i) apoCIII-siRNA-, (ii) control-siRNA-, and (iii) vehicle-treated, as a control for both apoCIII- and control-siRNA-treated mice. Through this randomization we ensured that all groups were equivalent from a glucometabolic point of view (Table 2). Mice were injected i.v. for three consecutive days with increasing doses of the apoCIII-siRNA mix and control-siRNA (Table 2). Vehicle-treated mice were given equivalent volumes of PBS (Invitrogen) (Table 2). BW was measured immediately before the injections to determine the dose. On the 4th day BW and BG were measured, mice were sacrificed and samples from blood, liver and intestine were collected. The effect of the different doses was evaluated at the gene expression level in liver and intestine

TABLE 2 Summary

Vehicle						
PBS						
Dilution factor	**[siRNA] (mg ml^{-1})**	**Body weight (g)**	**Volume injected (µl)**	**Dosage (µg)**	**Dosage (mg kg^{-1})**	**Blood glucose (mmol L^{-1})**
N/A	0	42.4 ± 1.8	160.0 ± 3.3	0	0	16.0 ± 1.9
Control-siRNA						
Stock concentration: 0.54 mg ml^{-1}						
1:4000	0.000135	45.5 ± 0.7	168.7 ± 1.7	0.02	0.0005	11.5 ± 0.3
1:800	0.000675	43.5 ± 2.0	161.0 ± 6.7	0.1	0.0025	9.3 ± 0.2
1:400	0.00135	39.9 ± 0.9	148.0 ± 4.9	0.2	0.005	11.6 ± 1.4
1:80	0.00675	44.9 ± 0.9	165.7 ± 2.9	1	0.025	18.5 ± 3.9
1:8	0.0675	41.3 ± 2.0	152.7 ± 8.2	10	0.25	15.0 ± 3.3
1:4	0.135	39.4 ± 2.0	145.7 ± 8.7	20	0.5	15.6 ± 0.8
1:2	0.27	40.2 ± 1.5	147.7 ± 6.2	40	1	15.1 ± 2.4
apoCIII-siRNA mix						
Stock concentration: 0.55 mg ml^{-1}						
1:4000	0.0001375	44.1 ± 1.0	161.3 ± 2.9	0.02	0.0005	12.5 ± 1.2
1:800	0.0006875	45.3 ± 0.9	166.7 ± 3.3	0.1	0.0025	11.2 ± 0.6
1:400	0.001375	40.9 ± 0.2	149.0 ± 1.0	0.2	0.005	10.4 ± 1.3
1:80	0.006875	45.3 ± 0.8	165.7 ± 2.9	1	0.025	13.9 ± 3.1
1:8	0.06875	40.1 ± 3.7	146.7 ± 14.5	10	0.25	15.6 ± 2.6
1:4	0.1375	39.6 ± 2.2	144.3 ± 8.7	20	0.5	17.4 ± 2.3
1:2	0.275	40.8 ± 1.1	146.7 ± 3.3	40	1	16.7 ± 4.2

Note: In the table are included the dilution factors of the siRNAs used for in vivo experiments, concentrations of siRNAs, volume of siRNAs injected, dosage in µg, dosage in mg kg^{-1} as well as body weight and non-fasting blood glucose levels of mice used in the concentration-response studies. Data are means ± SEM.

and at the protein level in liver and plasma. Dose–response curves are presented using a semi-logarithmic plot and analyzed by nonlinear regression modeling.

2.4.4 | Target dose determination and in vivo testing

Potency of the apoCIII-siRNA mix was determined on the basis of the IC$_{50}$ and efficacy by the I_{max}. These data were used to determine the optimal dose (target dose) where beneficial metabolic effects are expected. Based on our previous experience, treating *ob/ob* mice with ASO, a 50%–60% reduction in hepatic apoCIII gene expression levels resulted in an improved glucometabolic profile.[12]

Nonlinear regression modeling followed by interpolation of a 50%–60% reduction in apoCIII levels estimated a concentration of 0.0022 mg ml^{-1} of the apoCIII-siRNA mix to give the desired reduction of the apolipoprotein. The average dose given to the mice was 160 µl which is equivalent to 0.008 mg kg^{-1} or 0.35 µg of the siRNA mix.

To test whether the calculated dose of the apoCIII-siRNA mix indeed silenced the apoCIII gene to the target level in vivo, mice were assigned to three groups: (i) apoCIII-siRNA-, (ii) control-siRNA-, and (iii) vehicle-treated. They were injected i.v. for three consecutive days with 0.35 µg of apoCIII-siRNA mix or control-siRNA. Vehicle-treated mice were injected with equivalent volumes of PBS. On the 4th day, mice were sacrificed and samples from blood, liver, and intestine were collected for determination of apoCIII gene expression and/or protein levels.

2.4.5 | Duration of the gene silencing effect by the siRNA mix

To evaluate duration of effect of the apoCIII-siRNA mix, blood samples for analyses of plasma apoCIII protein levels were collected from the tail vein before the first dose (time point 0) and thereafter regularly until day 37 after the last dose.

2.4.6 | Long-term administration of apoCIII-siRNA mix

To study long-term effects mice were treated with 0.35 μg of siRNAmix or control siRNA for three consecutive days, every 15 days, for nine weeks. Non-fasting BW and BG were measured during daytime and blood samples were taken regularly during the study for analysis of apoCIII. At the end tests evaluating plasma LPL activity, glucose tolerance and insulin secretion were performed. Blood samples were collected for analysis of apoCIII, lipids, alanine aminotransferase (ALT), aspartate aminotransferase (AST), creatinine, creatine kinase activity and troponin I. After sacrificing the mice tissue samples from liver and intestine were collected.

2.4.7 | Species-specific activity of the apoCIII-siRNAs

Species specificity of the apoCIII-siRNA mix was tested in 40 days old DPBB rats. One day before the first administration of the siRNAs, rats were weighed and non-fasting BG was measured to randomize and distribute them into three different groups: (i) apoCIII-siRNA-, (ii) control-siRNA-, and (iii) vehicle-treated DPBB rats. The substances were given i.v for three consecutive days at a dose of 1 mg kg^{-1} (150 μg). BW was measured before the injection to calculate the correct dose. One day after the last injection, BW and BG were measured, rats were euthanized and samples were collected for analysis of apoCIII.

2.5 | RNA isolation, cDNA preparation and quantitative real-time PCR

Tissues (liver and intestine) were quickly dissected out, snap-frozen in liquid nitrogen and stored at −150°C until use. Total RNA was isolated using the RNeasy Lipid Tissue Mini Kit, according to the manufactures protocol (Qiagen). On-column digestion of DNA was performed during RNA purification using RNase-Free DNase I set (Qiagen). Total RNA concentrations were determined using a NanoPhotometer P330 (IMPLEN). One μg of total RNA was used for cDNA preparation using the Maxima First Strand cDNA Synthesis Kit (ThermoFisher), following manufacturer's instructions. qRT-PCR was performed in a QuantStudio 5 PCR system thermal cycler (Applied biosystems) with Power-Up SYBR green PCR master mix (Applied biosystems). Hepatic and intestinal apoCIII gene expression was determined. Off-target effects of the siRNAs were evaluated by measuring gene expression of

apolipoprotein AI, AIV and AV and angiopoietin-like-peptide 3, 4, and 8 in samples from liver and intestine. As control genes for liver target transcripts we used *β-actin*, TATA-binding protein (*TBP*), and Hypoxanthine Phosphoribosyltransferase 1 (*HPRT*); and for intestine target transcripts, *HPRT*, Beta-2-Microglobulin (*B2M*) and hydroxymethylbilane synthase (*HMBS*). Analysis of gene expression was done with the ΔΔCt method. The relative transcript levels of each target gene were normalized to each control gene and to the geometric mean of the cycle threshold (Ct) of all control genes used for qRT-PCR analyses in liver and intestine. The results are expressed as mRNA levels relative to vehicle- and/or control-siRNA-treated mice. Primer sequences are available in Table 3.

2.6 | Western blot analysis

Circulating apoCIII was determined in plasma. For hepatic apoCIII, liver samples were homogenized in ice-cold buffer containing 0.42 mmol L^{-1} NaCl, 20 mmol L^{-1} Hepes (pH 7.9), 1 mmol L^{-1} Na$_4$P$_2$O$_7$, 1 mmol L^{-1} ethylenediamine tetraacetic acid (EDTA), 1 mmol L^{-1} ethylene glycol tetraacetic acid (EGTA), 1 mmol L^{-1} dithiothreitol (DTT), 20% (vol/vol) glycerol, 20 mmol L^{-1} sodium fluoride, 1 mmol L^{-1} Na$_3$O$_4$V and Hal protease and phosphatase inhibitor cocktail (1:100). Tubes containing homogenates were exposed to thermal shock at −80°C in liquid nitrogen and thawed to 37°C in a water bath three consecutive times. Thereafter, homogenates were centrifuged at 10,000 × g for 20 min at 4°C, and supernatants collected. Protein concentrations were determined by Bradford assay (BioRad). Equal amounts of protein (50 μg for plasma and 25 μg for liver) were loaded onto a 4%–12% Bis-Tris gel (Invitrogen). For immunoblotting, membranes were blocked with 5% (wt/vol) bovine serum albumin (BSA) in 0.1% (vol/vol) Tween-20 (Sigma–Aldrich) in PBS (PBS-T). After blocking, membranes were probed overnight with either a rabbit polyclonal anti-apoCIII primary antibody (1:200; LSBio). After incubation with anti-rabbit IgG–peroxidase complexes for apoCIII protein determination (1:4000 for plasma and 1:2000 for liver; GE Healthcare), membranes were exposed to commercially enhanced chemiluminescence reagents (ClarityTM Western ECL Substrate, BioRad), and blots developed in a luminescent image analyzer (ChemiDocTM Touch Imaging System, BioRad). Transferrin was used as control protein in membranes loaded with plasma by using a rabbit polyclonal anti-transferrin primary antibody (1:1000; LSBio). Anti-rabbit IgG–peroxidase complexes (GE Healthcare) for transferrin detection were used at 1:4000 dilution. β-actin was selected as a control protein in membranes loaded with

TABLE 3 Sequences of the primer pairs used in the current study

Gene ID	Primer strand	Primer sequence (5′ → 3′)	PCR size (bp)
angptl3	Forward	CCGACTGCTCTGCCGTTTAT	115
	Reverse	CATGGACTGCCTGATTGGGTA	
angptl4	Forward	TTTGCAGACTCAGCTCAAGG	154
	Reverse	TCCATTGTCTAGGTGCGTGG	
angptl8	Forward	GATCCAGCAGAGACTCCACAC	191
	Reverse	CTTGCTTCTGTCTCCGCTCT	
apoAI	Forward	GCGGCAGAGACTATGTGTCC	75
	Reverse	CAGTTTTCCAGAGATTCAGG	
apoAIV	Forward	ACCCAGCTAAGCAACAATGC	88
	Reverse	TGTCCTGGAAGAGGGTACTGA	
apoAV	Forward	AACCGAGCAGGGGCCAT	170
	Reverse	TTCTCCTGTGCCAGCTTCTG	
apoCIII	Forward	CGCTAAGTAGCGTGCAGGA	68
	Reverse	TCTGAAGTGATTGTCCATCCAG	
ATGL	Forward	GGTCCTCCGAGAGATGTGC	75
	Reverse	TGGTTCAGTAGGCCATTCCTC	
β-Actin	Forward	CTAAGGCCAACCGTGAAAAG	104
	Reverse	ACCAGAGGCATACAGGGACA	
b2m	Forward	ATGCTGAAGAACGGGAAAAA	112
	Reverse	CAGTCTCAGTGGGGGTGAAT	
Cpt-1α	Forward	CTATGCGCTACTCGCTGAAGG	124
	Reverse	GGCTTTCGACCCGAGAAGA	
HMBS	Forward	CGGAGTCATGTCCGGTAAC	82
	Reverse	GGTGCCCACTCGAATCAC	
HPRT	Forward	CAGTCCCAGCGTCGTGATTA	167
	Reverse	GGCCTCCCATCTCCTTCATG	
HSL	Forward	TCCTCAGAGACCTCCGACTG	135
	Reverse	ACACACTCCTGCGCATAGAC	
LDL-R	Forward	GACCGCAGCGAGTACACCA	67
	Reverse	TCACCTCCGTGTCGAGAGC	
LRP-1	Forward	GGACCACCATCGTGGAAA	61
	Reverse	TCCCAGCCACGGTGATAG	
PPAR-α	Forward	AGAGCCCCATCTGTCCTCTC	153
	Reverse	ACTGGTAGTCTGCAAAACCAAA	
SREBP-1c	Forward	ATGCCATGGGCAAGTACACA	91
	Reverse	ATAGCATCTCCTGCGCACTC	
TBP	Forward	TGCTGTTGGTGATTGTTGGT	97
	Reverse	CTGGCTTGTGTGGGAAAGAT	

liver samples by using a mouse monoclonal anti-β-actin primary antibody (1:8000; Sigma–Aldrich). Anti-mouse IgG–peroxidase complexes (GE Healthcare) for β-actin detection were used at 1:10,000 dilution. Obtained images were quantified using the ImageJ software (NIH).

2.7 | Hematoxylin and eosin (H&E) staining in liver

Liver histology was evaluated in mice from the long-term treatment with siRNAs. At the end of the study, the left lobe

of the liver was quickly dissected out, rinsed in PBS to remove the excess of blood, snap-frozen in liquid nitrogen and preserved at −80°C until use. Liver sections (30 μm-thick) were obtained in a cryostat (Microm HM500M/ Cryostar NX70, Thermo Fisher Scientific) and collected onto SuperFrost Plus microscope slides (VWR International). After 1 h equilibrating at room temperature slides were rinsed in PBS for 1 min, fixed in 4% paraformaldehyde for 10 minutes, immersed in hematoxylin (Sigma–Aldrich) for 6 min, washed with distilled water, and stained with eosin (HistoLab) for 1 min. After staining, slides were dried at room temperature and mounted using a permanent mounting medium (Vector Laboratories). Once the mounting medium was solidified, the preparations were imaged under 5× and 10× magnification objectives (zoom 1.5×) using an optical microscope (Leica). The morphological evaluations were performed in sections from five individual animals per group. For each section, three fields of view were collected under the 10× magnification objective.

2.8 | Liver triglycerides content

The left lobe of the liver was dissected out, weighed, snap-frozen in liquid nitrogen, and stored at −80°C until use. Hepatic Tgs content was determined, as previously described,[35] by carcass saponification in 0.1 mol L^{-1} KOH in absolute ethanol. Tgs were analyzed using Free Glycerol Reagent and Glycerol Standards (Sigma–Aldrich) to construct the standard curve. The glycerol concentration (triolein equivalents) was measured by spectrophotometry (Envision 2103 Multilabel Reader, PerkinElmer) at $\lambda = 540$ nm and determined by extrapolation from the standard curve. Total Tgs content was expressed as mg per g of liver tissue.

2.9 | Intraperitoneal glucose tolerance test (IPGTT)

For glucose tolerance tests, mice from the long-term studies were fasted for 6 h during daytime. Blood glucose concentrations were measured at basal (0 min) and 10, 30, 60, and 120 min after an intraperitoneal (i.p.) injection of glucose (2 g kg^{-1} BW), as previously described.[22,36] Glucose was measured with an Accu-Chek Aviva meter (Roche Diagnostics Scandinavia AB). Blood samples were collected at all-time points for determination of insulin.

2.10 | Lipoprotein lipase activity

Mice, fasted for 6 h during daytime, were anesthetized with isoflurane and blood samples collected. Thereafter

they received an i.v injection of heparin (0.2 units per g BW) to release LPL from endothelial cells. Blood samples were collected 5, 10, and 15 min post-heparin injection into capillary tubes (Microvette CB 300 K2 EDTA tubes; SARSTEDT AG & Co. KG) and centrifuged at 3000 × g for 15 min at 4°C using a cold microcentrifuge (Eppendorf). Supernatants were collected and transferred to clean microtubes (Eppendorf). LPL activity was measured in plasma before and after heparin injection by a fluorimetric assay, according to manufacturer's instructions (Abcam). Standards, samples, background control (double distilled H$_2$O), positive control and negative control, together with the reaction mix, were loaded in duplicate into black 96-well plates. The plates were pre-incubated for 10 min at 37°C protected from light to stabilize the signal. Fluorescence intensity ($\lambda_{Ex}/\lambda_{Em} = 482/515$ nm) was measured in a kinetic mode every 10 min for 150 min using a fluorimeter (Envision 2103 Multilabel Reader, Perkin Elmer). Plasma LPL activity was determined, according to manufacturer's instructions, using the following equation:

$$\text{LPL activity} = \left(\frac{S}{\Delta T \times V}\right) \times D = \frac{\text{pmol}}{\text{ml/min}} = \text{mIU/min}$$

S is the amount of substrate in the sample well calculated from standard curve (pmol). ΔT is the reaction time (min) of two given time points in the linear range of the kinetic reading. V is the original sample volume added into the reaction well (ml). D is the sample dilution factor. To determine specific LPL activity in plasma, values from plasma LPL activity at time point 0 (pre-heparin i.v. injection) were subtracted from all time points analyzed, according to manufacturer's instructions. Data were corrected by the amount (μg) of total plasma proteins loaded per well in the sample wells, measured by Bradford's method.

2.11 | Creatine kinase activity

Creatine kinase activity was determined in plasma samples by a coupled enzyme reaction resulting in the production of NADPH proportional to the creatine kinase activity in the sample. In this reaction, phosphocreatine and ADP are converted to creatine and ATP. The ATP generated is used by hexokinase to phosphorylate glucose present in the plasma samples, thus resulting in glucose-6-phosphate. Subsequently, glucose-6-phosphate is oxidized by NADP in the presence of glucose-6-phosphate dehydrogenase to produce NADPH and 6-phospho-D-gluconate. Activity of creatine kinase was determined by spectrophotometry (Envision 2103 Multilabel Reader, PerkinElmer) at $\lambda = 340$ nm.

Plasma creatine kinase activity was determined, according to manufacturer's instructions (Merk), using the following equation:

$$\text{creatine kinase activity}$$
$$= \frac{(\text{ABS})\text{final} - (\text{ABS})\text{initial}}{(\text{ABS})\text{calibrator} - (\text{ABS})\text{blank}} \times 600$$
$$= \text{IU/L}$$

ABS is absorbance; the factor 600 is the equivalent activity (IU L^{-1}) of the calibrator when assay is read at 20 and 25 min; and one IU of creatine kinase is the amount of enzyme that transfers 1 μmol of phosphate from phosphocreatine to ADP per minute at pH 6.0. Data were corrected by the amount (μg) of total plasma proteins loaded per well, measured by Bradford's method.

2.12 | Plasma biochemistry

For biochemical determinations in plasma, blood samples were collected in Microvette CB 300 K2 EDTA tubes (SARSTEDT AG & Co. KG) and kept on ice. Thereafter, blood samples were centrifuged at $5000 \times g$ for 30 min at 4°C, supernatant containing plasma collected and preserved at −80°C until use. Insulin was analyzed using ultrasensitive mouse insulin enzyme-linked immunosorbent assay (ELISA) Kits (Crystal Chem, Inc.). AST and ALT were measured with mouse-specific commercial ELISA kits (MyBiosource). Creatinine concentrations were determined by a coupled enzyme reaction, which resulted in a colorimetric product, whose ABS was measured at $\lambda = 570$ nm using a spectrophotometer (Envision 2103 Multilabel Reader, Perkin Elmer). Troponin I was measured in plasma samples using a mouse-specific commercial ELISA kit (CUSABIO). Plasma triglycerides (Tgs) were analyzed by a colorimetric assay that uses the enzymatic hydrolysis of Tgs by the action of the lipase to produce glycerol and free fatty acids (Cayman). The glycerol produced was subsequently used by a coupled enzymatic reaction system, involving glycerol kinase, glycerol phosphate oxidase and peroxidase. The coupled reaction system resulted in a purple-colored product whose ABS was measured at $\lambda = 540$ nm using a spectrophotometer (Envision 2103 Multilabel Reader, Perkin Elmer). Plasma Tgs were calculated by extrapolating the ABS values from the standards. Plasma LDL- and HDL-cholesterol were determined by the Trinder reaction using colorimetric assays based in a modified polyvinyl sulfonic acid (PVS) and polyethylene-glycol methyl ether (PEGME) coupled classic precipitation method (Crystal Chem). These colorimetric assays resulted in a colored product whose ABS was measured at $\lambda = 620$ nm using a spectrophotometer (Envision 2103 Multilabel Reader, Perkin Elmer). Plasma LDL- and HDL-cholesterol were calculated by extrapolating the ABS values from the standards.

2.13 | Statistical analyses

The number of animals and group sizes used were estimated by power analyses using the G*Power 3.1 software,[37] based on our own pilot study and from results in published articles of similar kinds.[38] As far as possible, studies were designed to generate groups of equal size. No outliers were identified in the reported experiments. Animals were randomly allocated to each group based on glucometabolic parameters, such as BW and BG, taken one day before starting the experiments. The experiments were not performed in a blinded manner because the measurements could not be affected by personal bias. For qRT-PCR and Western blot analyses, the mean values of the control group were normalized to 1. Data are presented as means $\pm$ SEM and means $\pm$ SD. Statistical analyses were performed using GraphPad Prism 5.0. Statistical comparisons between two groups were performed using the non-parametric two-tailed Mann–Whitney U t-test. One-way analysis of variance (one-way ANOVA) followed by Tukey's post-hoc test was used when comparing three groups. Concentration-response curves involving multiple doses and groups were analyzed by two-way ANOVA followed by Bonferroni's post-hoc test. Statistical significance was defined as $p < 0.05$. Statistical analyses were undertaken only for studies in which each group size was at least $N = 5$. The declared group sizes in the current study represent the number of independent values, and data analyses were performed using these independent values.

3 | RESULTS

3.1 | ApoCIII gene silencing in vitro

Starting from the only 527 bp short mouse apoCIII mRNA (NM_023114.4), 390 siRNA candidates could be generated that perfectly match all four transcript variants deposited in NCBI RefSeq and are also directed against another four of the six transcript variants from the Ensembl database. Among these candidates, 24 siRNAs were identified that were predicted to be active and specific for mouse apoCIII.

As no cell line could be identified that expressed sufficient levels of endogenous apoCIII, we applied the

DualGlo reporter assay system for analyzing the knock-down activity of the selected siRNAs. This assay system expresses the target of interest in the 3′UTR of renilla luciferase, thus allowing to measure target knockdown by monitoring luciferase activity. A second luciferase expressed from the same plasmid was used for normalization. Twenty-four siRNAs targeting murine apoCIII were initially tested in a dual dose screen at 20 nmol L^{-1} and 0.2 nmol L^{-1}. Out of these, the best eight siRNAs were further analyzed in a 10 concentration dose–response experiment, starting at 50 nmol L^{-1} in 5-fold dilution steps down to 25 fmol L^{-1} (Figure 1A,B and Figure S1A–F). The best two siRNAs were very close in performance (Figure 1A,B), and thus were combined into one LNP formulation, in order to minimize potential molecule-specific side effects.

The siRNAs were formulated in a clinically applicable LNP based on the Axolabs' proprietary cationic lipid XL10[31] which can effectively deliver siRNAs to hepatocytes in vivo.[30,39] The LNPs have a mean particle diameter of 86 nm and a PDI of 0.05. The LNP exhibited a neutral surface charge of −0.1 mV. The siRNA concentration was 0.5 mg ml^{-1} and the drug encapsulation efficiency was 95% as measured using a ribogreen assay.

3.2 | Dose-dependent silencing of apoCIII in vivo

Before starting the treatment experiments, we confirmed that untreated 12-week-old male and female *ob/ob* mice had similar BW, BG, plasma insulin and Tgs, and that there was no difference in apoCIII gene expression in liver and intestine (Figure S2A–F). Thereafter, another cohort of mice of both sexes were given increasing concentrations of apoCIII-siRNA mix or control-siRNA i.v for three consecutive days (Figure S2G; Table 2). Vehicle-treated mice were used as control for both treatment groups. The apoCIII-siRNA mix induced a dose-dependent decrease in expression of liver apoCIII (Figure 1C,D). The effect was potent and there was a half-maximum reduction at a concentration that was more than 200-fold lower than the maximal inhibitory concentration (Figure 1C,D). The effect was confirmed at the protein level in liver (Figure 1E,F) and plasma (Figure 1G,H). No changes were seen in control-siRNA and in vehicle-treated mice (Figure S2H–J).

3.3 | Liver and species-specific effects

The siRNAs used in this study are designed to be liver specific and to ensure this, the expression of apoCIII in duodenum, the second largest source of apoCIII in rodents and humans, was analyzed.[40–42] None of the concentrations affected the intestinal expression of apoCIII (Figure 2A,B).

Species-specificity was evaluated in DPBB rats injected for three consecutive days with the highest dose tested, that is, 1 mg kg^{-1} BW (Figure 2C). Although the sequence similarity between rat and mouse apoCIII is about 80% no difference was observed in gene expression levels (Figure 2D) thereby confirming a mouse specific effect. BW and BG remained unchanged (Figure 2E,F).

3.4 | Off-target effects

The *apoCIII* gene resides within a gene cluster with *apoAI-apoAIV-apoAV* and knock-down of apoCIII can potentially affect LPL-dependent genes, such as *angptl3*, *angptl4*, and *angptl8*. To ensure that the siRNAs did not affect the expression of these genes they were determined in both liver and intestine and none of the doses of the siRNA mix affected any of them (Figure 3A–F, Figure S3A–F).

3.5 | ApoCIII-siRNA mix effects on different organs and triglycerides

To evaluate if there were any acute effects on plasma transaminases (ALT and AST), creatinine, creatine kinase activity and troponin I, as readouts for liver, kidney, muscle and heart, samples were taken from mice that had received the highest dose of the siRNA mix (Table 2) for three consecutive days. None of these parameters differed from samples taken from control animals (Figure 3G–K).

Lowering apoCIII is known to reduce Tgs in both rodents and humans.[12,20–22] In samples taken after a three-day treatment session the levels of Tgs were already lower than in control mice (Figure 3L), while there were no changes in plasma LDL- and HDL-cholesterol (Figure 3M,N).

## 3.6 | Target dose determination and duration of apoCIII lowering effect

For therapeutic silencing the aim, based on previous studies, was to reduce the levels of apoCIII by 50–60%.[12] From the dose–response curves 0.35 μg or 0.008 mg kg^{-1} of apoCIII-siRNA mix was chosen as the dose that was expected to result in the desired
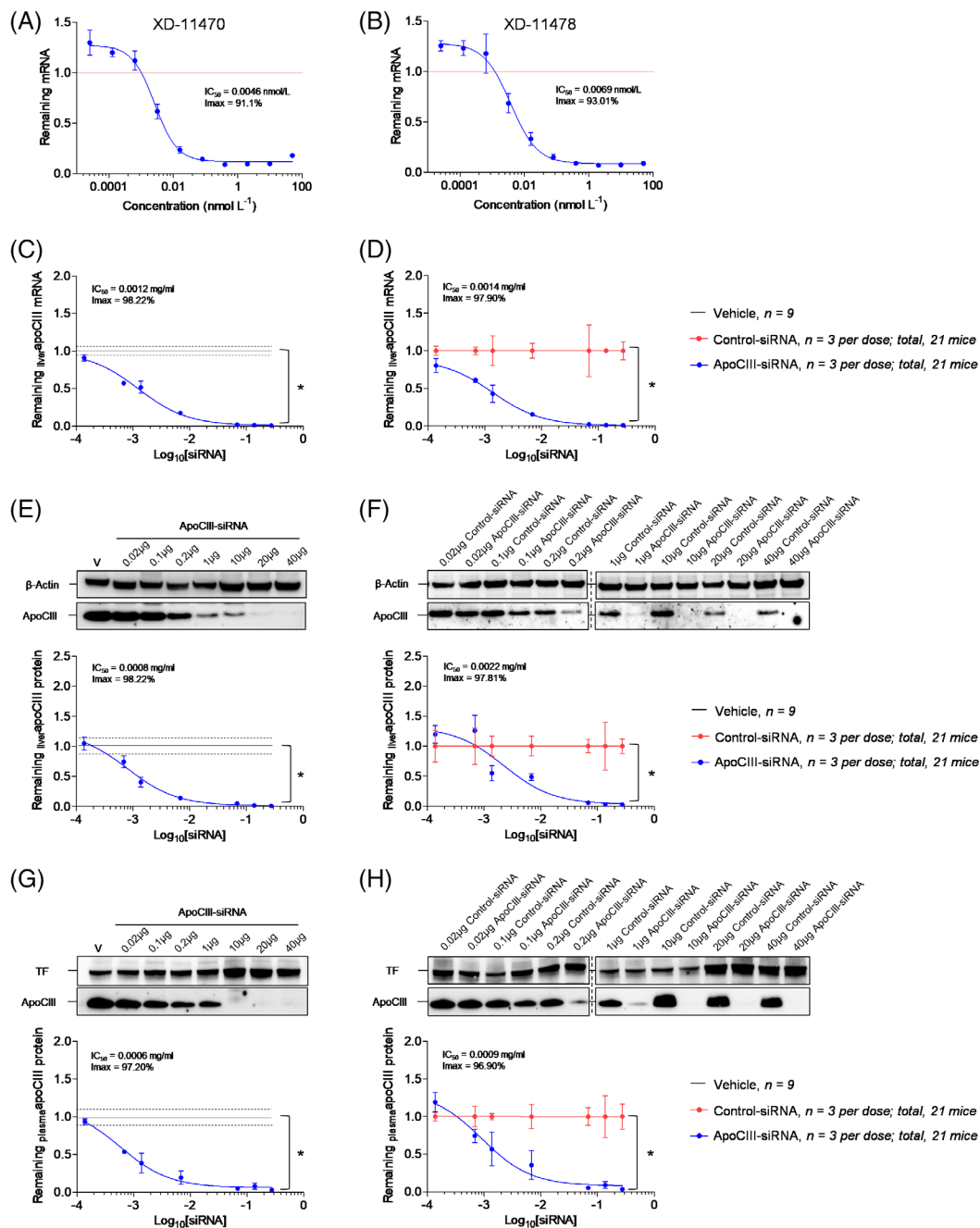
FIGURE 1 ApoCIII-siRNAs dose-dependently reduce apoCIII in vitro and in vivo. The two best (XD-11470 and XD-11478) out of eight siRNAs were tested in Hepa1-6 cells by co-transfection with a reporter plasmid expressing apoCIII in the 3′UTR of renilla luciferase (A,B). Luciferase signal was measured after 24 h incubation time and signal from mock-treated cells was set as 1. $N = 6$ in quadruplicate, data shown are means ± SD. *Ob/ob* mice were given i.v. injections of increasing concentrations of apoCIII-siRNA mix, control-siRNA ($N = 3$ individual animals for each dose) or vehicle ($N = 9$) for three consecutive days. (C,D) Expression levels of liver apoCIII in apoCIII-siRNA mix compared to (C) vehicle and (D) control-siRNA-treated mice. (E–H) Representative immunoblots and densitometry analysis of apoCIII in liver from siRNA mix treated mice compared to mice treated with (E) vehicle and (F) control-siRNA and in plasma from siRNA mix treated mice compared to mice treated with (G) vehicle and (H) control-siRNA. Data shown are means ± SEM. *$p < 0.05$, significantly different as indicated

reduction (Figure 1C–H). The theoretical dose estimation was consistent with the in vivo results, where three consecutive doses of the calculated amount of

siRNA mix reduced liver apoCIII gene expression and protein levels with $54.7 \pm 3.5\%$ and $41.9 \pm 10.5\%$, respectively (Figure 4A,B). Plasma samples, taken
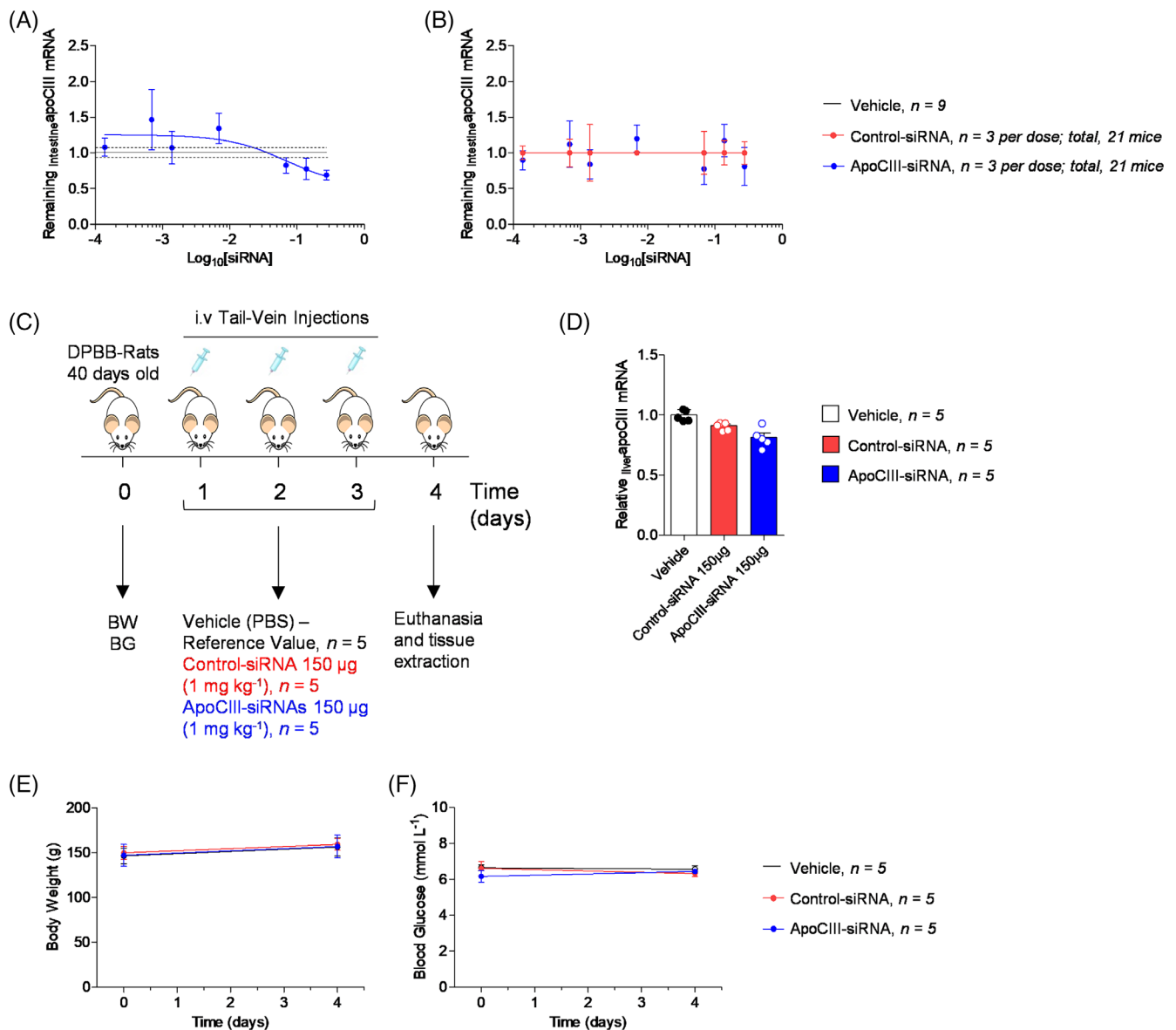
FIGURE 2 Tissue and species specificity. (A,B) ApoCIII mRNA levels in intestine from mice treated with increasing concentrations of apoCIII-siRNA mix ($N = 3$ individual animals for each dose) compared to (A) vehicle ($N = 9$) and (B) control-siRNA ($N = 3$ individual animals for each dose). Data shown are means ± SEM. (C) Experimental design for testing in DPBB rats. (D) ApoCIII mRNA levels in liver. (E) Body weight determined before and after treatment. (F) Blood glucose measured before and after treatment. Data shown are means ± SEM, $N = 5$

directly after the treatment session, showed a less pronounced decrease, $31.4 \pm 5.1\%$ compared to controls (Figure 4C). However, continued follow-up for 37 days, after the last injection, revealed that there was a progressive decrease in circulating apoCIII reaching the desired 50% level after around 8–12 days (Figure 4D,E). Three weeks after the last injection apoCIII had returned to the pretreatment level (Figure 4E). From these results, we decided to choose 15 days as the time interval between treatments with our siRNA mix.

## 3.7 | Long-term treatment with siRNAs against apoCIII improved metabolic derangements in *ob/ob* mice

O*b/ob* mice were treated every second week during nine weeks (Figure S4A). Plasma levels of apoCIII showed an initial progressive decrease and then remained stably lower compared to the controls (Figure 5A). As apoCIII inhibits LPL we did a functional test and this confirmed that LPL activity was higher in the siRNA mix treated mice (Figure 5B). This led to a decrease in plasma Tgs
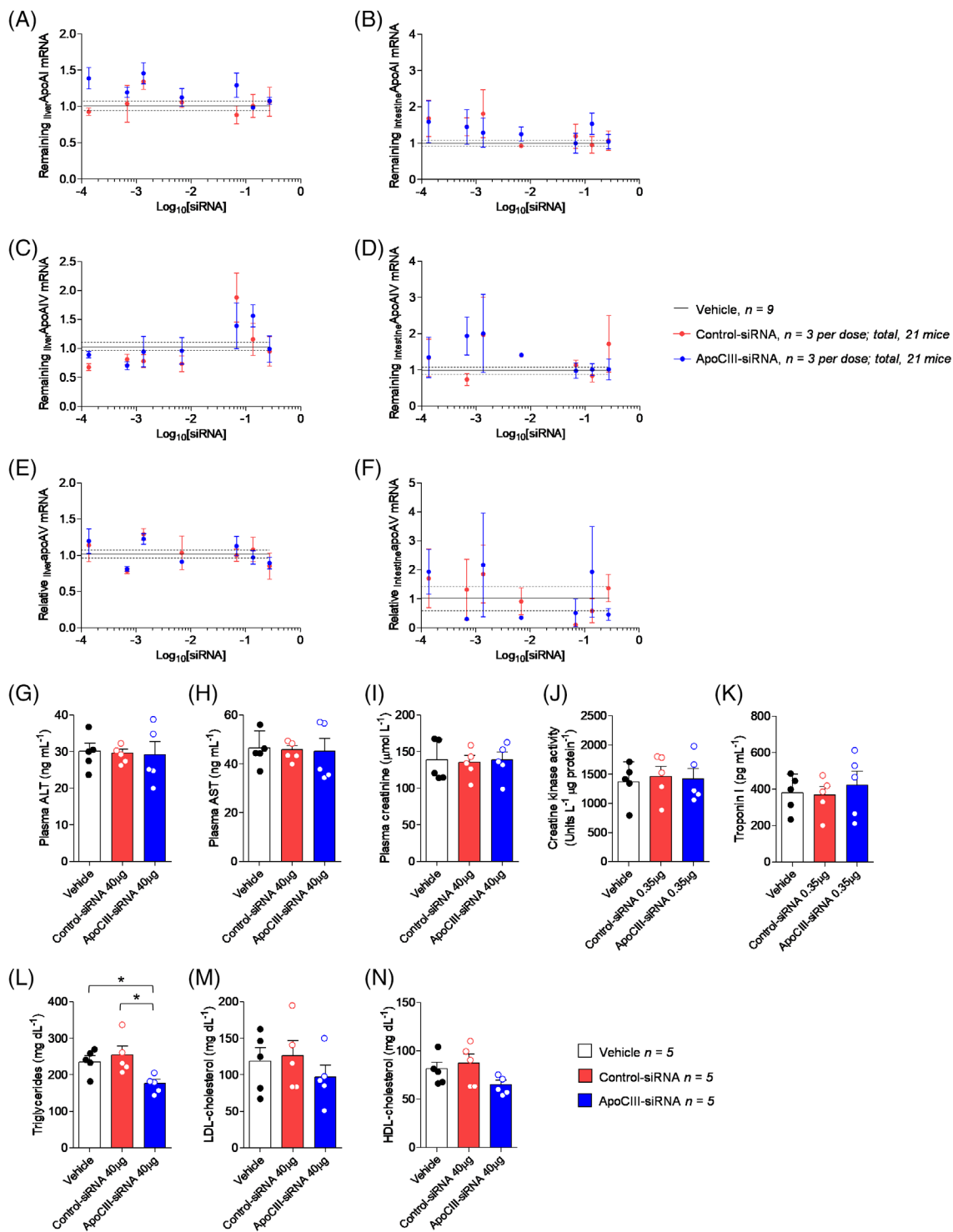
FIGURE 3 No unintended acute effects. Off-target effects were evaluated by measuring the expression levels of *apoAI*, *apoAIV*, and *apoAV*, respectively in (A,C,E) liver and (B,D,F) intestine. Data shown are means ± SEM; $N = 3$ individual animals for each dose of apoCIII-siRNA mix or control-siRNA, and $N = 9$ for vehicle. Plasma levels of (G) ALT, (H) AST, (I) creatinine, (J) creatine kinase activity, (K) troponin I, (L) Tgs, (M) LDL-cholesterol, and (N) HDL-cholesterol. Data shown are means ± SEM; $N = 5$. *$p < 0.05$, significantly different as indicated

without affecting plasma LDL- and HDL-cholesterol (Figures 5C and S4B,C). The LDL-cholesterol levels show a tendency to be lower, although not reaching statistical significance, in the siRNA treated animals (Figures 3M and S4B). These data are in line with previous observations that the strongest effect of lowering
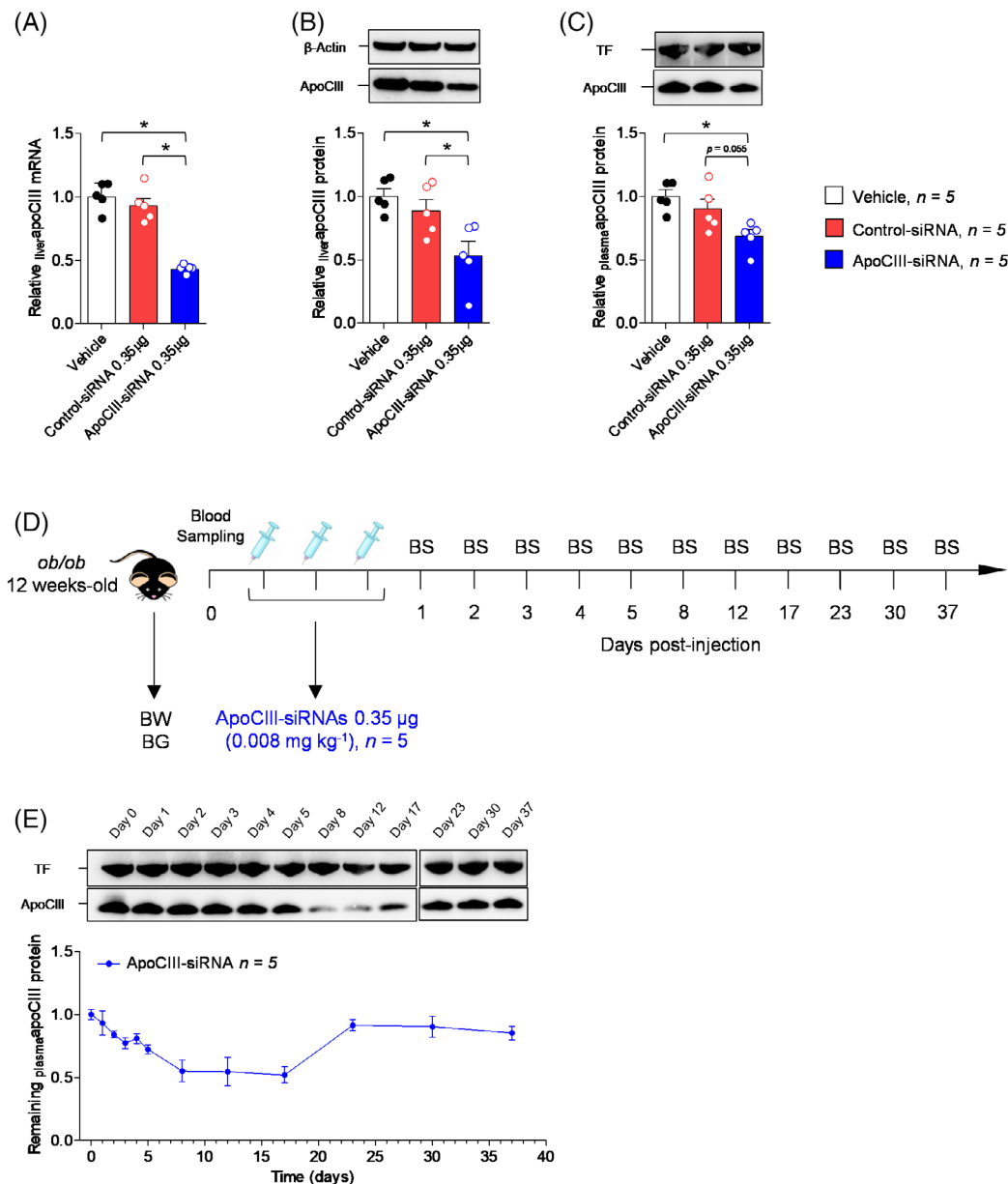
FIGURE 4 Evaluation of estimated target dose and duration of effect. (A) ApoCIII mRNA levels in liver. ApoCIII protein levels in (B) liver and (C) plasma. All samples were taken after three injections of the target dose of apoCIII-siRNA mix, control-siRNA or vehicle. (D) Protocol for determining the duration of effect. (E) Samples for plasma apoCIII measurements were taken before (baseline) and at indicated time points after the last i.v. injection of the apoCIII-siRNA. ApoCIII levels were normalized to baseline. For all graphs, data shown are means ± SEM, $N = 5$. *$p < 0.05$, significantly different as indicated

apoCIII is on the triglyceride-rich lipid particles.[12,20–22] At the end of the study, we confirmed that apoCIII gene and protein levels were reduced in liver, but not in duodenum (Figures 5D,E and S4E). There was an up-regulation of the hepatic lipoprotein receptors [LDL-receptor (*LDL-R*) and LDL-R-related protein 1 (*LRP-1*)] (Figure 5F), which might contribute to an increased removal of lipids from the circulation. In addition, there was an increased expression of the intracellular lipases adipose triglyceride lipase (*ATGL*) and hormone

sensitive lipase (*HSL*), as a sign of enhanced liver lipid catabolism, and of *PPAR-α* and carnitine palmitoyltransferase 1 a (*Cpt-1a*) that are involved in β-oxidation (Figure 5G,H). The observed improvements, together with the repression of genes involved in liver *de novo lipogenesis*, sterol regulatory element-binding protein 1 (*SREBP-1c*), fatty acid synthase (*FAS*) and acetyl-soenzyme A carboxylase (*ACC*), improved liver morphology (Figure 5I,J) and reduced hepatic fat accumulation in mice treated with the apoCIII-siRNA as compared to
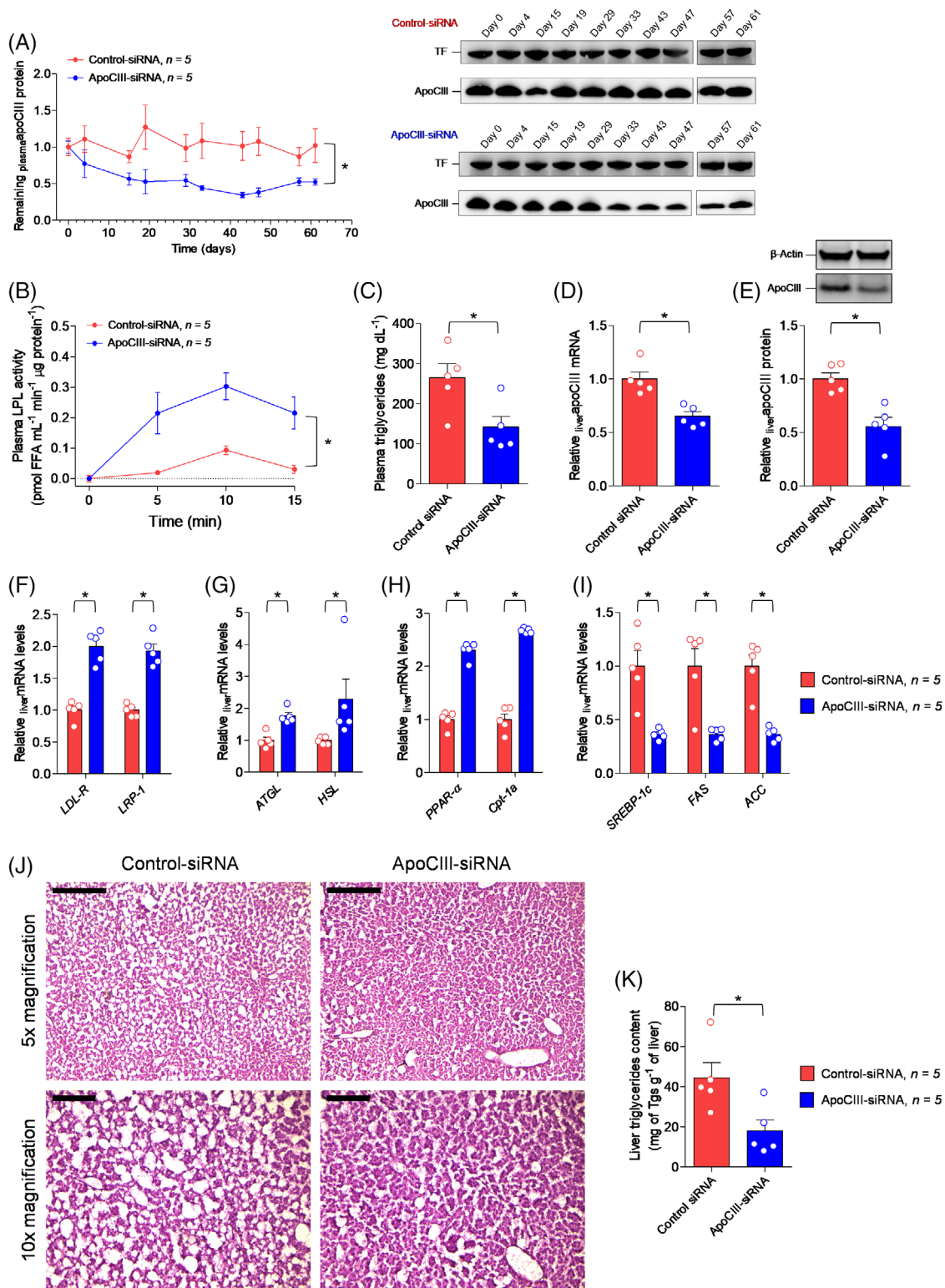
FIGURE 5 Long-term silencing of apoCIII increased LPL activity, lowered plasma Tgs and reduced liver fat accumulation. (A) Determination of circulating apoCIII protein levels at the indicated time points. Plasma (B) LPL activity and (C) Tgs at the end of the experiment. (D) Liver apoCIII mRNA and (E) representative immunoblots and densitometry analysis of liver apoCIII at the end of the experiment. (F–I) Relative liver gene expression levels of (F) *LDL-R* and *LRP-1*, (G) *ATGL* and *HSL*, (H) *PPAR-α* and *Cpt-1a*, (I) *SREBP-1c*, *FAS* and *ACC* by qRT-PCR. (J) Microphotographs of H&E stained liver sections from mice treated with control-siRNA (top left, 5× magnification; bottom left, 10× magnification) and apoCIII-siRNA (top right, 5× magnification; bottom right, 10× magnification). Scale bar in the top left corner of each microphotograph is 500 μm when the 5× magnification objective and 200 μm when the 10× magnification objective was used. (K) Liver triglycerides content. Data shown are means ± SEM, N = 5. *$p < 0.05$, significantly different as indicated
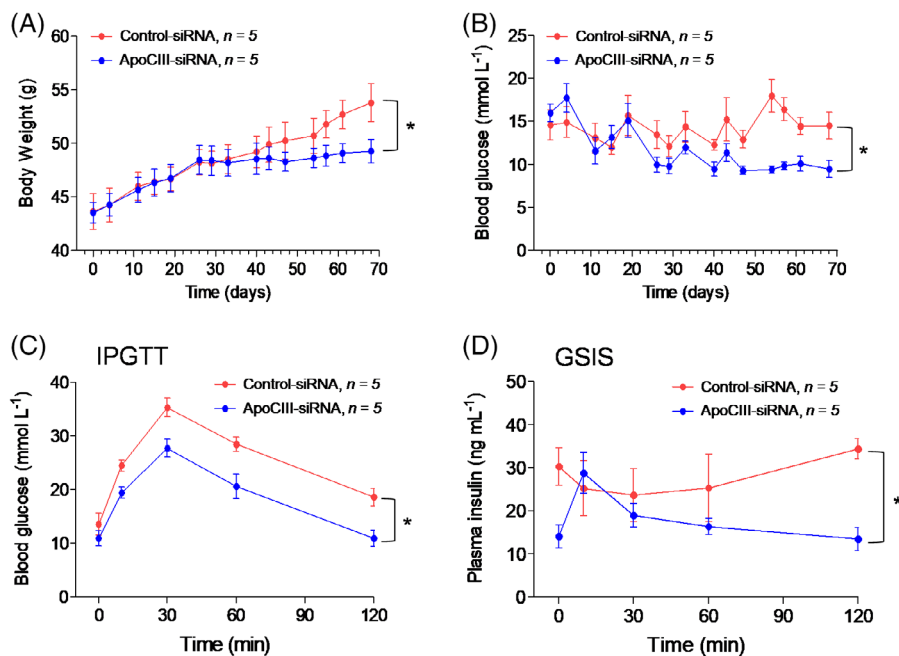
FIGURE 6 Long-term silencing of apoCIII resulted in improved body weight, glycemic control and insulin sensitivity. (A) Development of body weight and (B) non-fasting blood glucose during the study. (C) IPGTT and (D) GSIS during IPGTT. Data shown are means ± SEM, $N = 5$. *$p < 0.05$, significantly different as indicated

control group (Figure 5K). Furthermore, the lower levels of apoCIII caused weight gain to cease and improved non-fasting glucose levels, which indicates a smaller food intake (Figures 6A,B and S4D). Dynamic tests also showed an improved glucose tolerance and glucose-stimulated insulin release (Figure 6C,D). Unintended effects, after this long-term treatment, were evaluated by measuring expression levels of the cluster genes *apoAI*, *apoAIV*, and *apoAV* and LPL-dependent genes *angptl3*, *angptl4*, and *angptl8* and, as after acute exposure to the siRNAs, none of them were altered (Figure S4E,F). Neither were there any changes in plasma ALT, AST, creatinine, creatine kinase activity or troponin I levels (Figure S4G−K).

4 | DISCUSSION

With the increasing number of patients suffering from CVD and obesity-induced diabetes there is a world-wide interest in finding more effective treatments. The solid knowledge that increased levels of apoCIII are related to these diseases has made it an interesting druggable target.[3,12,20–22,43–46]

Further support for targeting apoCIII is that humans with loss-of-function mutations in the apoCIII gene, resulting in life-long lower apoCIII levels, are healthier and live longer.[47–49]

RNA therapeutics, initiated more than 40 years ago,[50] have the potential to specifically target disease-related genes and there are already drugs in clinical use based on this technology.[28,51,52]

4.1 | Development of siRNA against apoCIII

Our purpose of developing siRNA against apoCIII was to investigate whether this treatment strategy can suppress apoCIII levels for an extended period of time without side-effects, and if this improves the metabolic status of obese diabetic mice in a similar way as ASO.[12,22]

Out of 24 in silico designed siRNA candidates two, based on evaluation in vitro in Hepa 1–6 cells, were selected to be tested in vivo. The strategy of combining two siRNAs was chosen as this divides the dose of each siRNA, and thereby the risk of molecule-specific side effects, in half. The siRNAmix was demonstrated to be both liver and species specific.

4.2 | siRNA lowers apoCIII more efficiently and with a longer duration than ASO

The in vivo results are encouraging as after administrating siRNAmix for three consecutive days, twice per month, during nine weeks, the suppression of the gene remained, so there was no evidence of loss of effect over time. In our previously published work,[22] where apoCIII was lowered with ASO, we have shown that by reducing apoCIII there is a shift in liver lipid metabolism toward ketogenesis and fatty acids are transferred to the ketogenic pathway and ketones are taken up and used by BAT. The metabolic improvements and thereby the

underlying mechanisms were consistent with those observed with long-term treatment with ASO with cessation of weight gain, improved insulin sensitivity and glucose tolerance, as well as lowering of liver and systemic Tgs.

There were no injection site reactions and treated animals did not differ from control mice. Plasma AST, ALT, creatinine, creatine kinase, and troponin I, were unaffected both in the acute and long-term treated mice. Furthermore, we did not detect any effect on the genes situated within the same gene cluster as apoCIII or in LPL-dependent genes.

Compared to ASO, the other RNA approach we have used to target the *apoCIII* gene,[12,22] the siRNA mix was more potent and long-lasting. The amount of substance needed to reach the target level of reduction was 25 mg kg^{-1} eight times per month for ASO and 0.024 mg kg^{-1} twice per month for siRNA mix. The advantage with ASO was that it was given i.p, while the route of administration for our siRNA is i.v.

4.3 | Clinical translatability

There are several challenges to deliver siRNAs to the target tissue as they are both easily excreted via the kidneys and degraded by circulating nucleases.[53] Numerous chemical modifications have been tested to increase the possibilities to use siRNAs for RNA drugs. Of approved siRNAs in clinical use patisiran (hereditary transthyretin amyloidosis) is given as a single i.v infusion every third week,[54] inclisiran (heterozygous familial hypercholesterolemia)

twice per year as a subcutaneous (s.c.) injection,[55,56] givosiran (acute hepatic porphyria) s.c once a month[57] and lumisiran (primary hyperoxaluria type 1) is administered by s.c. injection once a month for three months, then monthly (BW < 10 kg), and quarterly for patients with a BW > 10 kg.[58]

Our next aims are to clarify whether one injection every second week will be enough to achieve the desired reduction in apoCIII, and to try to develop chemical formulations that will allow s.c. injections, with hopefully longer intervals between treatments. This seems possible as givosiran, like our siRNA against apoCIII is targeting the liver, and this drug is given as a s.c injection 12 times per year.

4.4 | Conclusion

The data in the present study demonstrate for the first time that i.v. administration of in silico designed siRNAs selectively and specifically silence mouse liver derived apoCIII with a higher potency and longer duration than previously tested ASO.[12,20,22] The metabolic improvements obtained after long-term treatment, together with the experience from already approved siRNAs used in the clinic, speaks in favor of that RNAi based therapeutics have the potential to become an apoCIII lowering drug (Figure 7).

AUTHOR CONTRIBUTIONS
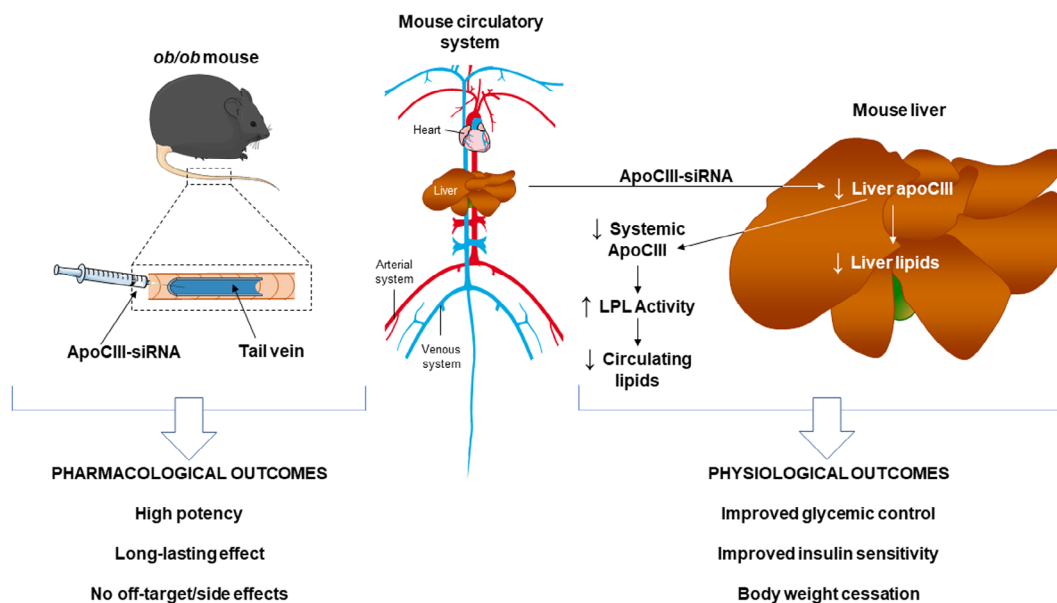
FIGURE 7 Schematic overview of the effects of treatment with apoCIII-siRNA

CONFLICT OF INTEREST
P. -O. B. is co-founder and CEO of Biocrine, a biotech company that is focusing on apoCIII as a potential drug target in diabetes. L. J. -B. is consult for the same company and has participated in advisory boards for NovoNordisk.

DATA AVAILABILITY STATEMENT
The data that support the findings of this study are available from the corresponding author upon reasonable request.

DECLARATION OF TRANSPARENCY AND SCIENTIFIC RIGOR
This declaration acknowledges that this article adheres to the principles for transparent reporting and scientific rigor of preclinical research as recommended by funding agencies, publishers, and other organizations engaged with supporting research.

ETHICS STATEMENT
All animal care and experiments were carried out according to the Animal Experiment Ethics Committee at Karolinska Institutet.

ORCID
Lisa Juntti-Berggren https://orcid.org/0000-0001-9690-4909

REFERENCES
1. Brown WV, Levy RI, Fredrickson DS. Studies of the proteins in human plasma very low density lipoproteins. J Biol Chem. 1969;244:5687–94.
2. Kohan AB. Apolipoprotein C-III: a potent modulator of hypertriglyceridemia and cardiovascular disease. Curr Opin Endocrinol Diabetes Obes. 2015;22:119–25.
3. Taskinen MR, Borén J. Why is apolipoprotein CIII emerging as a novel therapeutic target to reduce the burden of cardiovascular disease? Curr Atheroscl Rep. 2016;18:59.
4. Ginsberg HN, Le NA, Goldberg IJ, Gibson JC, Rubinstein A, Wang-Iverson P, et al. Apolipoprotein B metabolism in subjects with deficiency of apolipoproteins CIII and AI. Evidence that apolipoprotein CIII inhibits catabolism of triglyceride-rich lipoproteins by lipoprotein lipase in vivo. J Clin Invest. 1986;78:1287–95.
5. Larsson M, Vorrsjö E, Talmud P, Lookene A, Olivecrona G. Apolipoproteins C-I and C-III inhibit lipoprotein lipase activity by displacement of the enzyme from lipid droplets. J Biol Chem. 2013;288:33997–4008.
6. Sacks FM. The crucial roles of apolipoproteins E and C-III in apoB lipoprotein metabolism in normolipidemia and hypertriglyceridemia. Curr Opin Lipidol. 2015;26:56–63.
7. Gordts PL, Nock R, Son NH, Ramms B, Lew I, Gonzales JC, et al. ApoC-III inhibits clearance of triglyceride-rich lipoproteins through LDL family receptors. J Clin Invest. 2016;126:2855–66.
8. Zewinger S, Reiser J, Jankowski V, Alansary D, Hahm E, Triem S, et al. Apolipoprotein C3 induces inflammation and organ damage by alternative inflammasome activation. Nat Immunol. 2020;21:30–41.
9. Manzato E, Zambon A, Lapolla A, Zambon S, Braghetto L, Crepaldi G, et al. Lipoprotein abnormalities in well-treated type II diabetic patients. Diabetes Care. 1993;16:469–75.
10. Juntti-Berggren L, Larsson O, Rorsman P, Ammälä C, Bokvist K, Wåhlander K, et al. Increased activity of L-type Ca^{2+} channels exposed to serum from patients with type I diabetes. Science. 1993;261:86–90.
11. Juntti-Berggren L, Refai E, Appelskog I, Andersson M, Imreh G, Dekki N, et al. Apolipoprotein CIII promotes Ca^{2+}-dependent beta cell death in type 1 diabetes. Proc Natl Acad Sci U S A. 2004;101:10090–4.
12. Åvall K, Ali E, Leibiger IB, Leibiger B, Moede T, Paschen M, et al. Apolipoprotein CIII links islet insulin resistance to β-cell failure in diabetes. Proc Natl Acad Sci U S A. 2015;112:E2611–9.
13. Zannis VI, Kan HY, Kritis A, Zanni E, Kardassis D. Transcriptional regulation of the human apolipoprotein genes. Front Biosci. 2001;6:D456–504.
14. Altomonte J, Cong L, Harbaran S, Richter A, Xu J, Meseck M, et al. Foxo1 mediates insulin action on apoC-III and triglyceride metabolism. J Clin Invest. 2004;114:1493–503.
15. Caron S, Verrijken A, Mertens I, Samanez CH, Mautino G, Haas JT, et al. Transcriptional activation of apolipoprotein CIII expression by glucose may contribute to diabetic dyslipidemia. Arterioscl Thromb Vasc Biol. 2011;31:513–9.
16. Chen M, Breslow JL, Li W, Leff T. Transcriptional regulation of the apoC-III gene by insulin in diabetic mice: correlation

with changes in plasma triglyceride levels. J Lipid Res. 1994;35: 1918–24.

17. Li WW, Dammerman MM, Smith JD, Metzger S, Breslow JL, Leff T. Common genetic variation in the promoter of the human apo CIII gene abolishes regulation by insulin and may contribute to hypertriglyceridemia. J Clin Invest. 1995;96: 2601–5.

18. Béliard S, Nogueira JP, Maraninchi M, Lairon D, Nicolay A, Giral P, et al. Parallel increase of plasma apoproteins C-II and C-III in Type 2 diabetic patients. Diabet Med. 2009;26:736–9.

19. Holmberg R, Refai E, Höög A, Crooke RM, Graham M, Olivecrona G, et al. Lowering apolipoprotein CIII delays onset of type 1 diabetes. Proc Natl Acad Sci U S A. 2011;108: 10685–9.

20. Graham MJ, Lee RG, Bell TA 3rd, Fu W, Mullick AE, Alexander VJ, et al. Antisense oligonucleotide inhibition of apolipoprotein C-III reduces plasma triglycerides in rodents, nonhuman primates, and humans. Circ Res. 2013;112:1479–90.

21. Gaudet D, Alexander VJ, Baker BF, Brisson D, Tremblay K, Singleton W, et al. Antisense inhibition of apolipoprotein C-III in patients with hypertriglyceridemia. N Engl J Med. 2015;373: 438–47.

22. Valladolid-Acebes I, Åvall K, Recio-López P, Moruzzi N, Bryzgalova G, Björnholm M, et al. Lowering apolipoprotein CIII protects against high-fat diet-induced metabolic derangements. Sci Adv. 2021;7:eabc2931.

23. Duivenvoorden I, Teusink B, Rensen PC, Romijn JA, Havekes LM, Voshol PJ. Apolipoprotein C3 deficiency results in diet-induced obesity and aggravated insulin resistance in mice. Diabetes. 2005;54:664–71.

24. Borén J, Packard CJ, Taskinen MR. The roles of ApoC-III on the metabolism of triglyceride-rich lipoproteins in humans. Front Endocrinol (Lausanne). 2020;11:474.

25. Bertrand J, Pottier M, Vekri A, Opolon P, Maksimenko A, Malvy C. Comparison of antisense oligonucleotides and siR-NAs in cell culture and in vivo. Biochem Biophys Res Commun. 2002;296:1000–4.

26. Miyagishi M, Hayashi M, Taira K. Comparison of the suppressive effects of antisense oligonucleotides and siRNAs directed against the same targets in mammalian cells. Antisense Nucleic Acid Drug Dev. 2003;13:1–7.

27. Li Z, Fortin Y, Shen SH. Forward and robust selection of the most potent and noncellular toxic siRNAs from RNAi libraries. Nucleic Acids Res. 2009;37:e8.

28. Watts JK, Corey DR. Silencing disease genes in the laboratory and the clinic. J Pathol. 2011;226:365–79.

29. Crooke ST, Witztum JL, Bennett CF, Baker BF. RNA-targeted therapeutics. Cell Metab. 2018;27:714–39. https://doi.org/10.1016/j.cmet.2018.03.004

30. Seitz S, Kwon Y, Hartleben G, Jülg J, Sekar R, Krahmer N, et al. Hepatic Rab24 controls blood glucose homeostasis via improving mitochondrial plasticity. Nat Metab. 2019;1:1009–26. https://doi.org/10.1038/s42255-019-0124-x

31. Constien R, Geick A, Hadwiger P, Haneke T, Ickenstein LM, Hernandez Prata CA, et al. Novel lipids and compositions for intracellular delivery of biologically active compounds. 2012. US 2012/0295832 A1; 2018.

32. Brachs S, Winkel AF, Tang H, Birkenfeld AL, Brunner B, Jahn-Hofmann K, et al. Inhibition of citrate cotransporter Slc13a5/mINDY by RNAi improves hepatic insulin sensitivity and prevents diet-induced non-alcoholic fatty liver disease in mice. Mol Metab. 2016;5:1072–82. https://doi.org/10.1016/j.molmet.2016.08.004

33. Görgens SW, Jahn-Hofmann K, Bangari D, Cummings S, Metz-Weidmann C, Schwahn U, et al. A siRNA mediated hepatic dpp4 knockdown affects lipid, but not glucose metabolism in diabetic mice. PLOS ONE. 2019;14:e0225835. https://doi.org/10.1371/journal.pone.0225835

34. Ziegler N, Raichur S, Brunner B, Hemmann U, Stolte M, Schwahn U, et al. Liver-specific knockdown of class iia hdacs has limited efficacy on glucose metabolism but entails severe organ side effects in mice. Front Endocrinol (Lausanne). 2020; 11:598. https://doi.org/10.3389/fendo.2020.00598

35. Norris AW, Chen L, Fisher SJ, Szanto I, Ristow M, Jozsi AC, et al. Muscle-specific PPARgamma-deficient mice develop increased adiposity and insulin resistance but respond to thia-zolidinediones. J Clin Investig. 2003;112:608–18. https://doi.org/10.1172/JCI17305

36. Paschen M, Moede T, Valladolid-Acebes I, Leibiger B, Moruzzi N, Jacob S, et al. Diet-induced β-cell insulin resistance results in reversible loss of functional β-cell mass. FASEB J. 2019;33:204–18. https://doi.org/10.1096/fj.201800826R

37. Faul F, Erdfelder E, Lang AG, Buchner A. G*Power 3: a flexible statistical power analysis program for the social, behavioral, and biomedical sciences. Behav Res Methods. 2007;39:175–91. https://doi.org/10.3758/bf03193146

38. Soutschek J, Akinc A, Bramlage B, Charisse K, Constien R, Donoghue M, et al. Therapeutic silencing of an endogenous gene by systemic administration of modified siRNAs. Nature. 2004;432:173–8. https://doi.org/10.1038/nature03121

39. Woitok MM, Zoubek ME, Doleschel D, Bartneck M, Mohamed MR, Kießling F, et al. Lipid-encapsulated siRNA for hepatocyte-directed treatment of advanced liver disease. Cell Death Dis. 2020;11:343. https://doi.org/10.1038/s41419-020-2571-4

40. Zannis VI, Cole FS, Jackson CL, Kurnit DM, Karathanasis SK. Distribution of apolipoprotein A-I, C-II, C-III, and E mRNA in fetal human tissues. Time-dependent induction of apolipoprotein E mRNA by cultures of human monocyte-macrophages. Biochemistry. 1985;24:4450–5. https://doi.org/10.1021/bi00337a028

41. Ogami K, Hadzopoulou-Cladaras M, Cladaras C, Zannis VI. Promoter elements and factors required for hepatic and intestinal transcription of the human ApoCIII gene. J Biol Chem. 1990; 265:9808–15. https://doi.org/10.1016/S0021-9258(19)38743-5

42. West G, Rodia C, Li D, Johnson Z, Dong H, Kohan AB. Key differences between apoC-III regulation and expression in intestine and liver. Biochem Biophys Res Commun. 2017;491:747–53. https://doi.org/10.1016/j.bbrc.2017.07.116

43. Adams D, Gonzalez-Duarte A, O'Riordan WD, Yang C-C, Ueda M, Kristen A, et al. Patisiran, an RNAi therapeutic, for hereditary transthyretin amyloidosis. N Engl J Med. 2018;379: 11–21. https://doi.org/10.1056/NEJMoa1716153

44. Gonzalez-Duarte A, Coelho T, Adams D, Yang C-C, Polydefkis M, Kristen A, et al. Long-term use of patisiran, an investigational RNAi therapeutic, in patients with hereditary transthyretin-mediated amyloidosis: 12 month efficacy and safety from global open-label extension study. Presented at:

AANEM Annual Meeting, National Harbor, MD, October 10–13, 2018. Abstract 10; 2018.

45. Adams D, Polydefkis M, González-Duarte A, Wixner J, Kristen AV, Schmidt HH, et al. Long-term safety and efficacy of patisiran for hereditary transthyretin-mediated amyloidosis with polyneuropathy: 12-month results of an open-label extension study. Lancet Neurol. 2020;20:49–59. https://doi.org/10.1016/S1474-4422(20)30368-9

46. Kim YK. RNA therapy: current status and future potential. Chonnam Med J. 2020;56:87–93. https://doi.org/10.4068/cmj.2020.56.2.87

47. Atzmon G, Rincon M, Schechter CB, Shuldiner AR, Lipton RB, Bergman A, et al. Lipoprotein genotype and conserved pathway for exceptional longevity in humans. PLoS Biol. 2006;4:e113. https://doi.org/10.1371/journal.pbio.0040113

48. Pollin TI, Damcott CM, Shen H, Ott SH, Shelton J, Horenstein RB, et al. A null mutation in human APOC3 confers a favorable plasma lipid profile and apparent cardioprotection. Science. 2008;322:1702–5. https://doi.org/10.1126/science.1161524

49. TG and HDL Working Group of the Exome Sequencing Project, National Heart, Lung, and Blood Institute, Crosby J, Peloso GM, Auer PL, Crosslin DR, et al. Loss-of-function mutations in APOC3, triglycerides, and coronary disease. N Engl J Med. 2014;371:22–31. https://doi.org/10.1056/NEJMoa1307095

50. Zamecnik PC, Stephenson ML. Inhibition of Rous sarcoma virus replication and cell transformation by a specific oligodeoxynucleotide. Proc Natl Acad Sci U S A. 1978;75:280–4. https://doi.org/10.1073/pnas.75.1.280

51. Jackson AL, Bartz SR, Schelter J, Kobayashi SV, Burchard J, Mao M, et al. Expression profiling reveals off-target gene regulation by RNAi. Nat Biotechnol. 2003;21:635–7. https://doi.org/10.1038/nbt831

52. Fedorov Y, Anderson EM, Birmingham A, Reynolds A, Karpilow J, Robinson K, et al. Off-target effects by siRNA can induce toxic phenotype. RNA. 2006;12:1188–96. https://doi.org/10.1261/rna.28106

53. Juliano R, Alam MR, Dixit V, Kang H. Mechanisms and strategies for effective delivery of antisense and siRNA oligonucleotides. Nucleic Acids Res. 2008;36:4158–71. https://doi.org/10.1093/nar/gkn342

54. Hoy SM. Patisiran: first global approval. Drugs. 2018;78(15):1625–31. https://doi.org/10.1007/s40265-018-0983-6

55. Fitzgerald K, White S, Borodovsky A, Bettencourt BR, Strahs A, Clausen V, et al. A highly durable RNAi therapeutic inhibitor of PCSK9. N Engl J Med. 2017;376:41–51. https://doi.org/10.1056/NEJMoa1609243

56. Raal FJ, Kallend D, Ray KK, Turner T, Koenig W, Wright RS, et al. Inclisiran for the treatment of heterozygous familial hypercholesterolemia. N Engl J Med. 2020;382:1520–30. https://doi.org/10.1056/NEJMoa1913805

57. Honor A, Rudnick SR, Bonkovsky HL. Givosiran to treat acute porphyria. Drugs Today (Barc). 2021;57(1):47–59. https://doi.org/10.1358/dot.2021.57.1.3230207

58. Garrelfs SF, Frishberg Y, Hulton SA, Koren MJ, O'Riordan WD, Cochat P, et al. Lumasiran, an RNAi therapeutic for primary hyperoxaluria type 1. N Engl J Med. 2021;2021384(13):1216–26. https://doi.org/10.1056/NEJMoa2021712

SUPPORTING INFORMATION

Additional supporting information can be found online in the Supporting Information section at the end of this article.

> **How to cite this article:** Recio-López P, Valladolid-Acebes I, Hadwiger P, Hossbach M, Krampert M, Prata C, et al. Treatment of the metabolic syndrome by siRNA targeting apolipoprotein CIII. BioFactors. 2022. https://doi.org/10.1002/biof.1885